Journal of Asian Earth Sciences 276 (2024) 106362

Contents lists available at ScienceDirect

Journal of Asian Earth Sciences

journal homepage: www.elsevier.com/locate/jseaes

Development of arcuate faults and controls on hydrocarbon accumulation in the Tiantai slope, Xihu Depression, East China Sea basin

Lang Yu [a,b], Yixin Yu [a,b,*], Yiming Jiang [c], Wei Zou [c], Gongcheng Zhang [d], Xianjun Tang [c], Ting Tang [a,b], Xinxin Liang [a,b], Xinjian He [c], Dongxia Chen [a,b]

[a] National Key Laboratory of Petroleum Resources and Engineering, China University of Petroleum, Beijing 102249, China
[b] College of Earth Sciences, China University of Petroleum, Beijing 102249, China
[c] CNOOC Shanghai Branch, Shanghai 200335, China
[d] CNOOC Research Institute Company Limited, Beijing 100028, China

ARTICLE INFO

Keywords:
Arcuate fault
Fault activity
Lateral sealing ability
Hydrocarbon accumulation
Tiantai slope
Xihu depression

ABSTRACT

The strike-slip movement of NW-trending transfer zone in the Tiantai slope of the Xihu Depression governed the development of the Cenozoic arcuate faults. These faults significantly influenced trap formation, sand-bodies distribution, and hydrocarbon migration. Based on seismic, drilling data and fault activity analysis methods, this paper describes the origin and evolution of the arcuate faults and their impact on hydrocarbon accumulation. These arcuate faults exhibit a change from NE to NW strike orientation in plan view, and are distributed in the hanging wall of the NW-trending basement faults. The main arcuate faults penetrate the bottom of the Cenozoic strata and extend upward through the top of the lower member of the Huagang Formation, markedly affecting the depositional dynamics of the Pinghu Formation. The segments of the arcuate faults began to grow during the Middle Eocene, and experienced hard linkages in the Late Eocene. The activity of these arcuate faults diminished significantly and gradually stopped during the Middle and Late Oligocene. The segmentation and linkage growth processes of the arcuate faults controlled the formation and evolution of traps. Additionally, the activities of these faults influenced the distribution of sandbodies, with the segmentation points of the arcuate faults serving as important conduits for sediment input. Moreover, the arcuate faults served as effective pathways for vertical hydrocarbon migration. The area with the arcuate faults present favorable conditions for hydrocarbon accumulation in the Tiantai slope of the Xihu Depression.

1. Introduction

Faults are fundamental elements in the analysis of petroleum basins and are recognized as crucial factors of hydrocarbon accumulation, due to their significant influence on hydrocarbon generation, migration, accumulation, and distribution (Luo and Bai, 1998). When studying the evolutionary mechanisms of discontinuous faults, Segall and Pollard (1980) proposed that these faults experienced segmentation growth processes, which subsequently lead to the formation of various types of hydrocarbon traps at different developmental stages (Wang et al., 2014). Additionaly, the activities of these faults can lead to regional thermal subsidence, maturation and evolutionary processes of source rocks (Sun et al., 2008). Variability in the activity across different segments of a single fault can alter provenance input and the direction of paleo-currents, therefore impacting distribution of reservoirs within the basin (Feng, 2006; Wan et al., 2013). Furthermore, faults can function as both migration pathways and seals for hydrocarbon accumulation during hydrocarbon exploration (Bense et al., 2003; Sample et al., 2006).

The Xihu Depression, located in the East China Sea Shelf basin in eastern China (Fig. 1a), is a proven hydrocarbon-rich depression. This depression has been influenced by multi-phase tectonic activities, resulting in a complex fault system characterized by various combinations of fault patterns (Zhang et al., 2014). Previous studies primarily concentrated on the developmental characteristics of this fault system and its implications for hydrocarbon accumulation within the Xihu Depression. It has been proposed that faults that developed during the rifting phase primarily served as conduits for hydrocarbon migration, whereas those that formed during the reversion stage played a crutial role in the formation of effective hydrocarbon traps (Cai et al., 2014; Cai and Zhang, 2013; Zhang, 2013). In addition, research concerning the

* Corresponding author.
E-mail address: yuyixin@cup.edu.cn (Y. Yu).

https://doi.org/10.1016/j.jseaes.2024.106362
Received 29 May 2024; Received in revised form 12 September 2024; Accepted 2 October 2024
Available online 3 October 2024

characteristics of fault systems in the Pinghu slope and their impact on hydrocarbon accumulation have been completed. In the northern region of the Pinghu slope, situated within the western slope belt of the Xihu Depression, and their influence on hydrocarbon accumulation had been completed. In the northern part of the Pinghu slope, a complex fault system were identified with a series of structural traps that have been significantly influenced by tension stress (Cai and Zhang, 2013; Zhang, 2013; Zhu et al., 2022). Moreover, a structural transfer zone has been documented in the Tiantai slope within the Xihu Depression, where its characteristics and formation mechanisms have been preliminary studied (Wang et al., 2020a). In the Tiantai slope, NW-trending extensional detachment faults in the Mesozoic strata facilitate accommodation and transfer functions for geological frameworks, fault development, and extensional intensities across the southern and northern parts of the slope during the Cenozoic (Wang et al., 2020a; Yu et al., 2023). The strike-slip movement of these NW-trending basement faults has resulted in the development of a series of arcuate faults on the hanging walls of the basement faults (Yu et al., 2023). The growth and development process of arcuate faults plays an important role in controlling hydrocarbon accumulation by influencing trap formation, the distribution sand-bodies, and hydrocarbon migration paths. Research conducted on the formation mechanisms of arcuate faults in the northern fault zone of the Enping Depression within the Pearl River Mouth Basin shows that these faults were formed due to the change in the direction of extensional stress from northwest to northeast (Wang et al., 2011). This formation was further influenced by the presence of a pre-existing thrust fault in the Mesozoic era. In the mean time, arcuate faults play a crucial role in controlling hydrocarbon accumulation within the northern fault step belt. As hydrocarbons migrate along the fault strike, the hanging wall demonstrates a higher efficiency in channeling hydrocarbons compared to the footwall (Wu et al., 2020). Previous studies on the genesis of the arcuate fault system in the southern slope zone of the Dongying Depression, Bohai Bay Basin, suggest that early faults gradually became inactive during the extensional process. As a result, new deformation zones, characterized by antithetic normal faults, are generated at the bending part of the faults, eventually forming the arcuate fault system (Ren et al., 2004). Similarly, the research in this paper provides valuable insights into the development characteristics and formation mechanisms of arcuate faults, which can serve as a reference for other regions. The northern part of the Tiantai slope is in proximity to the Pinghu oil and gas field, with both areas situated east of the primary hydrocarbon-supplying depression (Wang et al., 2020a), indicating promising exploration potential. Notably, while several commercial oil and gas field have been discovered in the Pinghu slope in the western slope zone of the Xihu Depression, no such fields have yet been discovered in the Tiantai slope. Therefore, an in-depth investigation into the development characteristics of arcuate faults in the Tiantai slope and their impact on hydrocarbon accumulation is crutial for advancing oil and gas exploration in this area. Utilizing the newest 3D seismic and drilling data, this study systematically analyzes the development and activity characteristics of the arcuate faults in the Tiantai slope, with a particular focus on their influence on trap formation, sandbody distribution, and hydrocarbon migration. The results show a strong correlation between the stages of trap formation and the timing of significant hydrocarbon generation and expulsion within the arcuate fault zone of the Tiantai slope. Additionally, the arcuate faults exhibit robust vertical migration abilities, which promotes favorable conditions for hydrocarbon accumulation in adjacent traps.

2. Geological setting

The NE-trending Xihu Depression, covering an area of approximately 5×10^4 km^2, is located within the eastern depression zone of the East China Sea Shelf basin, where the Cenozoic sedimentary strata exceeds 15,000 m in thickness (Fig. 1a) (Zhou, 2020). The tectonic configuration of the Xihu Depression is strongly influenced by underlying basement faults, resulting in a structural pattern characterized by north–south zonation and east–west partitioning. The depression can be subdivided into the western slope belt, central inversion structural belt and eastern fault terrace belt from west to east (Fig. 1b).

Since the Mesozoic era, the Xihu Depression has experienced four main evolutionary stages: the faulted basin stage, the fault-depression transition stage, the depression and reversion stage, and the regional subsidence stage (Zhou et al., 2019; Jiang et al., 2020; Wang et al.,

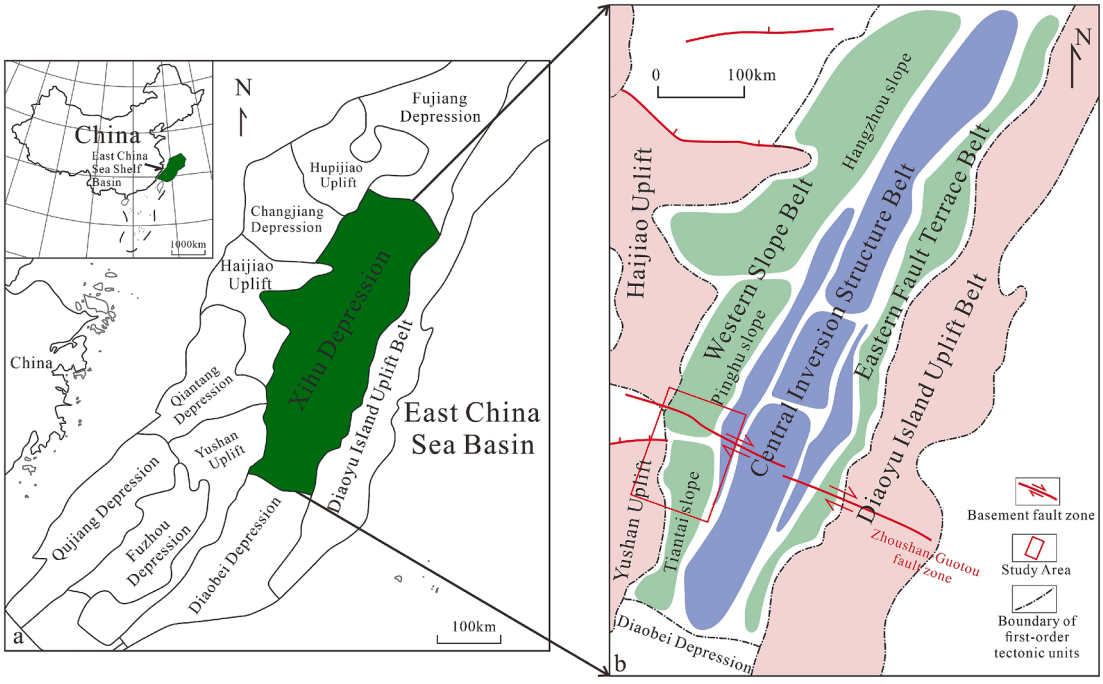

Fig. 1. (a) Location of the East China Sea Shelf basin in China and structural units of the basin. The green area is the Xihu Depression; (b) Division of structural units of the Xihu Depression. The study area is outlined by the red box (after Wang et al., 2020a; Wang et al., 2021).

2021). The basement of the Xihu Depression is primarily composed of a substantial volume of metamorphic and igneous rocks, with localized occurrences of Mesozoic-Paleozoic formations. The metamorphic basement is predominantly composed of sedimentary metamorphic rocks, while the igneous basement is largely characterized by granite intrusions (Taira et al., 1982; Jiang et al., 2020). Overlying these basement rocks, the Xihu Depression is dominated by Cenozoic clastic sedimentation. Stratigraphically, this includes the Eocene Bajiaoting-Baoshi-Pinghu formations, the Oligocene Huagang Formation, the Longjing-Yuquan-Liulang formations, the Pliocene Santan Formation, and the Pleistocene Donghai Formation (Wang et al., 2020a; Zou et al., 2021; Zhang et al., 2023; Liang et al., 2024) (Fig. 2). From the Late Cretaceous to the Early Eocene, the subduction direction of the Izanagi plate shifted, and the movement of the Pacific plate began to influence the South China region (Clague and Dalrymple, 1989; Suo et al., 2012). During this period, the East China Sea Shelf basin was subjected to the NW-SE extensional stress, initiating its evolution into a faulted basin (Yu et al., 2018). During the Late Eocene, the subduction direction of the Pacific plate had changed from NNW to NWW (Suo et al., 2012; Wilson, 2016), leading to a transition from extensional to compressional stress. This change weakened the fault activity, exerting minimal influence on sedimentation processes. Consequently, the intensity of faulted depression significantly decreased, marking the basin's transition into the fault-depression conversion satge (Zhou et al., 2019; Li et al., 2016). Following the Yuquan movement in the Late Eocene, extensional activity in the Xihu Depression had largely ceased, giving way to regional compression. This shift marked the beginning of the depression evolution stage, during which the Huagang Formation was deposited (Zhou et al., 2019; Yu et al., 2018). From the Pliocene to the present, the East China Sea Shelf basin has undergone regional subsidence (Yu et al., 2018; Li et al., 2016), a process attributed to the eastward migration of the spreading zone of the Okinawa trough (Wu et al., 2004).

The Tiantai slope is located in the southern part of the western slope zone of the Xihu Depression, and is surrounded by the Pinghu slope to the north, the Yushan uplift to the west, and the central inversion tectonic zone to the east (Fig. 1b). Gravity and magnetic data reveal that the presence of several NW-trending basement fault zones in the East China Sea Shelf basin, including the Hupi Reef fault, the Middle Ryukyu fault, the Hunan-Baodao fault, the Zhoushan-Guotou fault, and the Yushan-Jiumi fault. The Zhoushan-Guotou fault zone, with a total length of about 700 km, extends from the Zhoushan Islands outside the Hangzhou Bay to the Guotou Island (Wang et al., 2020a; Yang et al., 2010). The fault zone can be subdivided into three segments, with the central segment intersecting the south-central part of the Xihu Depression (Fig. 1b) (Jiao, 1988; Yang et al., 2010; Wang et al., 2020a). The Zhoushan-Guotou fault is a shovel-type normal fault inclining to the NE, and cut the basement downward and the Paleocene upward in cross section. It has been suggested that the Zhoushan-Guotou fault zone is not only a pre-existing fault zone in the basement, also has important influence on the tectonic framework of the northern and southern parts of the Xihu Depression (Wang et al., 2020a). In response to the influence of the NW-trending Zhoushan-Guotou fault zone, several NW-trending basement faults developed in the Tiantai slope. These faults have served as accommodation and transferring roles, supporting the development of NE- and NNE-trending faults system during the Cenozoic and accommodating the differential extensional stresses between the southern and northern parts. Consequently, some faults adjacent to the NW-trending basement faults have altered their trends, exhibiting an arcuate configuration in plan view.

Influenced by multi-stage tectonic movements, the Tiantai slope developed three groups of faults with different orientations, mainly consisting of NE-trending faults, followed by NNW- and NW-trending

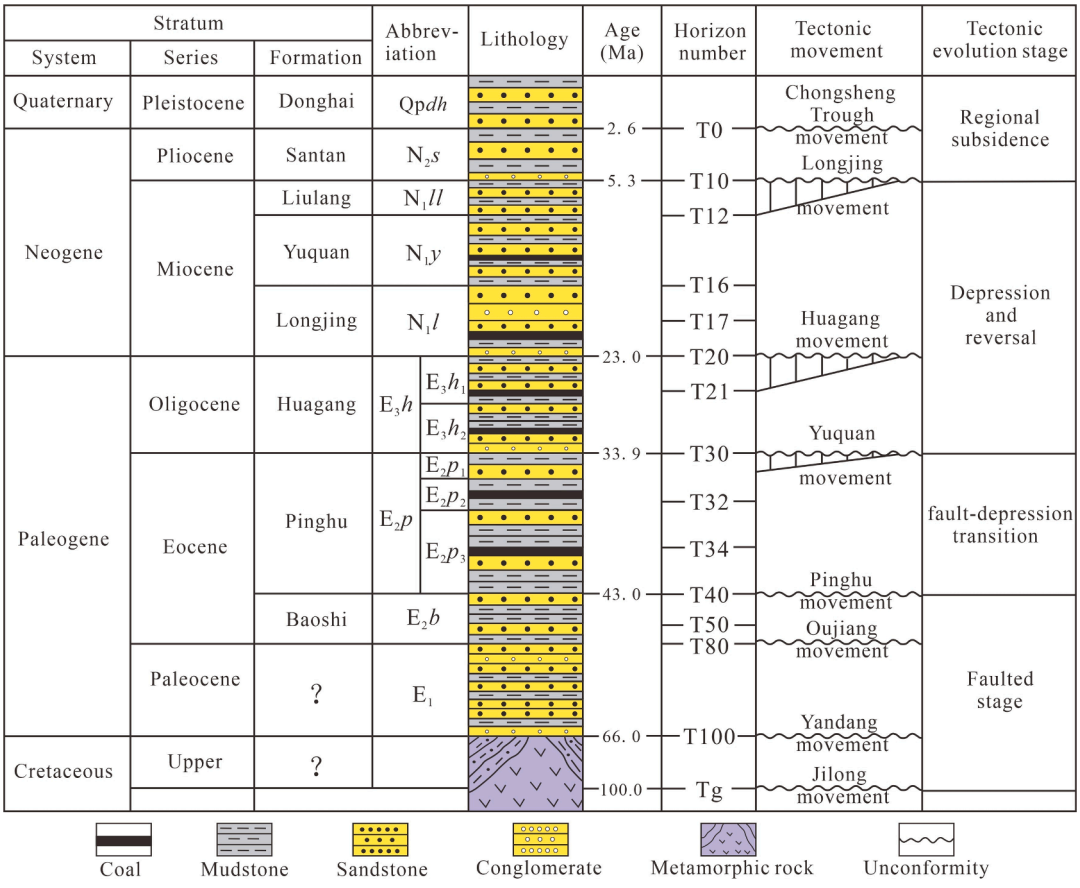

Fig. 2. Generalized tectonostratigraphic column showing the lithology, major sequences, and evolution stages in the Xihu Depression (after Wang et al., 2020a).

faults. During the Middle to Late Mesozoic, a few NW-striking basement normal faults in response to NE-SW extension stress. During the Paleocene-Early Eocene era, the Tiantai slope was influenced by the NW-SE extension, leading to large-scale faulted depression activities and the development of NE-NNE trending faults. Since the Late Oligocene, the Tiantai slope has been subjected to NW-SE compression, and most of the NE-trending faults were inactive, with only a few near EW-trending faults developing in the east.

3. Data and methods

3.1. Seismic and well data

Three-dimensional (3D) seismic data from 2017 and drilling data from the Shanghai Oil Company Ltd. CNOOC, were used in this research. The new 3D seismic data encompasses the entire Tiantai slope (Fig. 1b) with an area of 2000 km^2 and inline, crossline, and vertical geometry sample intervals of 25 m, 12.5 m, and 2 ms, respectively. The predominant frequency in the 3D seismic data is ~24 Hz. Additionally, The well data are from four exploratory wells, namely, A1, A2, A3, and A4, which are located within the Tiantai slope (Fig. 3). All the wells have vertical seismic profile (VSP) data. These high-quality seismic and well data facilitated the detailed interpretion of arcuate faults in the Tiantai slope.

3.2. Fault growth patterns and activity analysis

Fault strike displacement-distance curves (Peacock and Sanderson, 1994; Fossen, 2010; Giba et al., 2012) are employed to identify growth and development patterns across the main arcuate faults F1, F2, and F3 of the Tiantai slope. As shown in Fig. 4a, fault displacement of different sedimentary periods is statistically analyzed along the fault strike, and the position where the displacement abruptly changes indicates the segment point of the fault development. The arcuate faults described herein originate from *syn*-sedimentary faults in the extensional regime. Therefore, the growth index and fault displacement buried depth curve are utilized to assess the intensity of fault activity in various geological periods. The growth index refers to the ratio of the of the hanging-wall thickness to the footwall thickness of a fault, and its value can be used to determine the main active period of the fault as well as the intensity of fault activity. An index exceeding 1 indicates that the fault was active

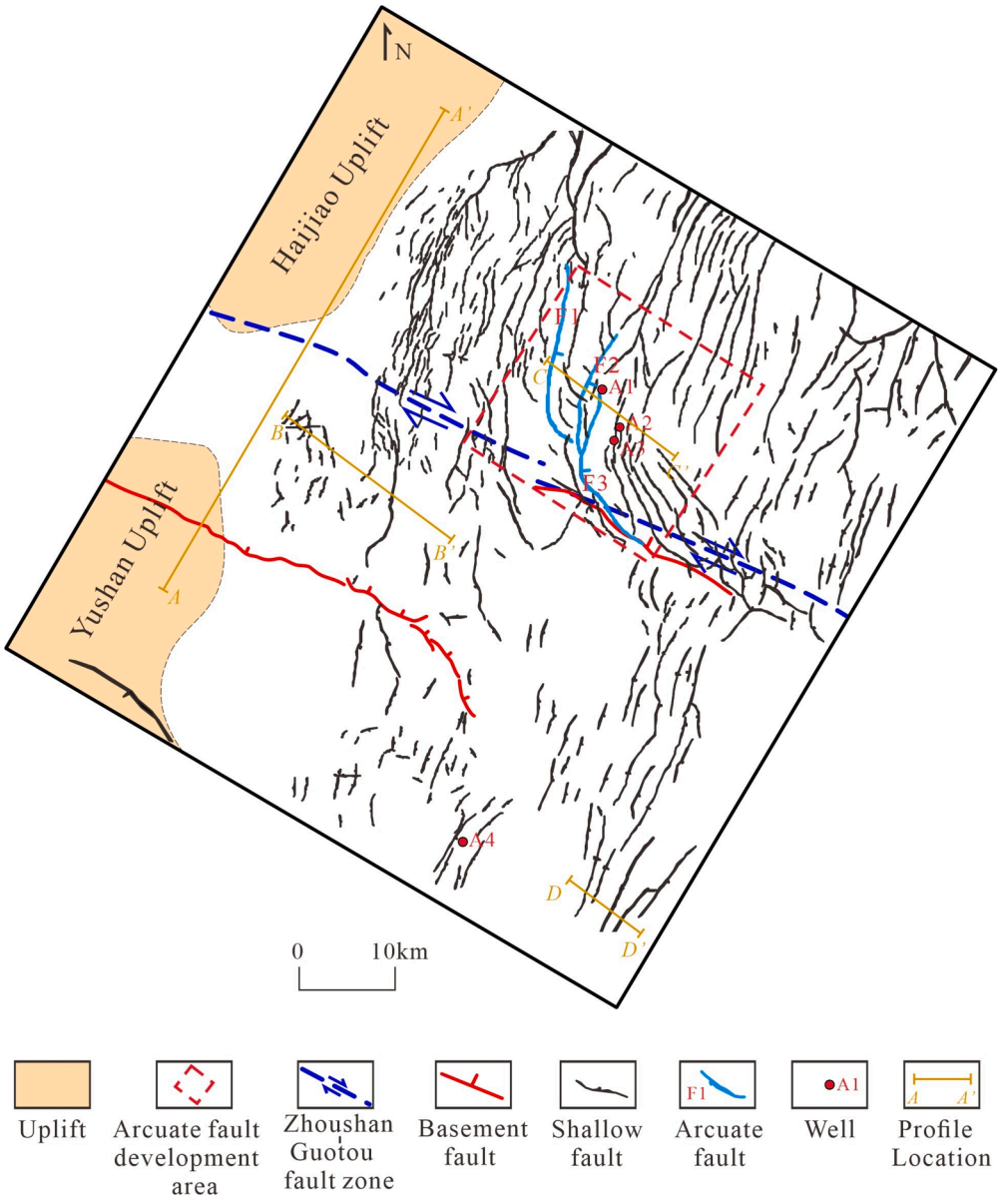

Fig. 3. Fault system of the T30 reflection layer at the top boundary of the Eocene Pinghu Formation on the Tiantai Slope.

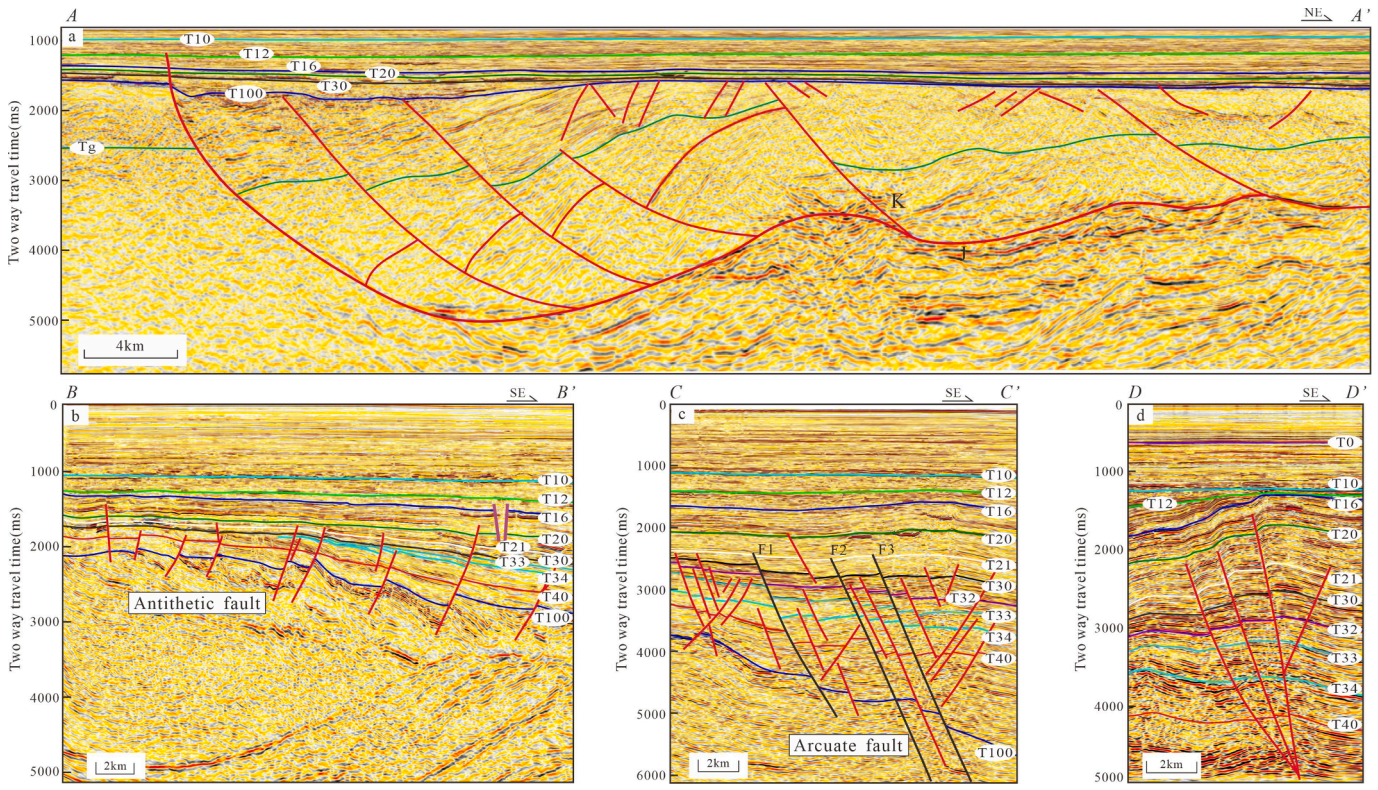

Fig. 4. Seismic profiles showing the basement faults (a), antithetic faults (b), arcuate faults (c), and strike-slip faults (d) in the Tiantai slope. See Fig. 3 for lines locations.

during that period, with larger values signifying stronger fault activity. Similarly, the fault growth index can also excludate the influence of faults on stratigraphic sedimentation.

3.3. Evaluation of lateral sealing capacity of fault

This study selects SGR (shale gouge ratio) to evaluate the lateral sealing capacity of arcuate faults. The SGR at a certain breakpoint is the ratio of the cumulative thickness of mudstone slipping through that point relative to the fault displacement (Yielding, et al, 1997). Using seismic interpretation results, the vertical fault displacement at each point of the arcuate faults F1, F2, and F3 is calculated. At the same time, shale content along the fault plane is calculated using well log data, and the SGR value of the fault plane is calculated using the SGR algorithm.

4. Results

The distinct tectonic position of the Tiantai slope in the Xihu Depression, where the NW trending basement fault zone passed through the slope area, led to significant differences in the slope structure between the southern and northern sides of the Tiantai slope (Wang et al., 2020a). Interpretations of seismic data show that the presence of three primary fault groups in the Tiantai slope, oriented in NE, NNW and NW directions (Fig. 3).

4.1. Arcuate faults characteristics

4.1.1. Arcuate faults plane distribution characteristics

During the Middle and Late Eocene, pre-existing NW-trending basement faults occurred dextral strike-slip movement (Yu et al., 2023), resulting in a shift of Cenozoic fault strikes from NE to NW. It is crutial to acknowledge that several arcuate faults are predominantly localized in the hanging wall of the basement faults. The arcuate faults exhibit a NE orientation in the northern sector and gradually change to NW in the south. Specifically, the arcuate fault F3 predominantly trends NE. In the hanging wall of arcuate fault F3, a series of secondary faults oriented NE, NNW and NW have developed. These secondary faults are mainly arranged in parallel and en echelon configurations, which are similar to the horsetail structures formed at the end of strike-slip faults (Fig. 3).

4.1.2. Deformation characteristics of arcuate faults profile

In the Tiantai slope, the basement faults are characterized as listric normal faults controlling the Mesozoic strata, which shows a structural pattern of half graben (Fig. 4a). Faults combinations in the Cenozoic strata involve synthetic and antithetic fault terraces. The NW-trending antithetic faults cut through the base Cenozoic (T100) downward and terminate upward at the upper member of the Huagang Formation (T20), which exhibits minimal influence on strata deposition (Fig. 4b). The majority of the faults in the Cenozoic cut upward through the upper member of the Pinghu Formation, with some fault activity persisting into the depositional stage of the Longjing Formation. Influenced by the strike-slipping movement of faults, the faults in the eastern Tiantai slope have the characteristics of flower structures in the profile. During the Longjing movement, the strata show a broad and gentle anticlinal shape influenced by the compression (Fig. 4b-d).

The arcuate faults are arranged parallel to each other in the profile and inclined to SE. The main arcuate faults F1, F2, and F3 cut downward through the basal Cenozoic strata and extend upward to the top of the lower member of the Huagang Formation. Notably, there are pronounced variations in the thickness of the Pinghu Formation on either side of these arcuate faults (Fig. 4c). In addition, several interlayer faults have developed among the arcuate faults, mostly located within the Pinghu Formation and show a Y-shaped pattern in the profile (Fig. 4c).

4.2. Activity histroies of arcuate faults

The growth of faults is a dynamic process and has different characteristics under varying tectonic and sedimentary environments (Liu,

2017). In general, there are two different models of fault growth and evolution, i.e., the isolated fault growth and segmentation growth (Segall and Pollard, 1980; Fossen et al., 2007). The activity characteristics of the arcuate faults display significant variability during different periods of the Cenozoic. Analysis of displacement-distance curves of the arcuate faults reveals that arcuate faults F1, F2, and F3 demonstrate characteristics of segmentation growth (Fig. 5).

The displacement-distance curve for the base of the lower and middle members of the Pinghu Formation shows a distinct segmentation point on the arcuate fault F1 (Fig. 5a). During the deposition of these members, fault F1 exhibited two discrete southern and northern segments, with the southern segment demonstrating more pronounced activity. As deposition progressed to the upper member of the Pinghu Formation, fault F1 transitioned into a integral fault with hard linkage, maintaining activity through the deposition of the upper member of the Huagang Formation. Similarly, arcuate fault F2 has a segmentation point, which can also be shown by the displacement-distance curve at the base Pinghu Formation (Fig. 5b). The middle sector of arcuate fault F2 showed greater activity intensity compared to its northern and southern ends, with the throw of the southern fault tapering to zero, indicating that growth of fault F2 initiated from the middle part and subsequently propagated towards both ends. Additionaly, the arcuate fault F3 has two segmentation points in the the displacement-distance curve of the top of the pre-Pinghu Formation and the lower member of the Pinghu Formation (Fig. 5c). This suggests that fault F3 was comprised of three segments with independent growth during the depositional periods of the pre-Pinghu Formation and the middle member of the Eocene Pinghu Formation.Subsequently, fault F3 exhibited growth with hard linkage and minimal displacement during the deposition of the upper member of the Pinghu Formation.

The growth index, defined as the ratio of the thickness of the hanging wall to that of the footwall, serves as a quantitative measure ascertain the key activity periods of activity and the intensity of fault movements (Wang et al., 2020b). Analysis of the displacement-buried depth curves and growth index curves of the arcuate faults reveals that faults F1 and F2 exhibit characteristics of continuous growth. Specifically, the fault throws of both F1 and F2 gradually increase from top to bottom, consistently demonstrating growth index values exceeding 1 (Fig. 6a and Fig. 6b). This indicates sustained fault activity through various stratigraphic levels. During other depositional periods, however, the activity of fault F1 was weak or entirely inactive. Similarly, the growth indices show that the arcuate fault F2 exhibited stronger activity during the depositional periods of the lower member, the middle and lower submember and the upper member of the Pinghu Formation. The displacement-burial depth curve for arcuate fault F3 reveals a maximum displacement point (Fig. 6c). Additionally, the growth indexs show that arcuate fault F3 became active during the depositional period of the middle member of the Pinghu Formation. The growth index for fault F3 reaches the maximum value during the depositional period of the upper member of the Pinghu Formation, indicating that fault F3 experienced its most intense activity during this time.

5. Discussion

5.1. Controls of arcuate faults on trap formation

The tectonic activities of the arcuate faults in the Cenozoic had mainly controlled the formation of structural traps in the Tiantai slope. These traps predominantly involve faulted block and faulted anticlinal traps, etc. (Fig. 7). As above stated, the arcuate faults in the Tiantai slope experienced three evolution stages, including the segmented growth in the Middle Eocene, hard-linkage growth in the Late Eocene, and a subsequent weakening of fault activity in the Oligocene. Arcuate faults F1 and F2 began to develop during the depositional period of the lower member of the Pinghu Formation, and reached the strongest activity during the depositional period of the upper member of the Pinghu Formation. Arcuate fault F3 initiated its development during the depositional period of the middle member of the Pinghu Formation, and reached its maximum activity during the depositional period of the upper member of the Pinghu Formation. The throw of arcuate fault F3 is significantly larger than that observed in arcuate faults F1 and F2, indicating that the activity intensity of the arcuate faults moved eastward gradually. The faulted block and faulted nose traps, controlled by the arcuate faults F1 and F2, mainly developed during the depositional periods of the upper member of the Pinghu Formation and the lower member of the Huagang Formation. These faults achieved hard linkage in the Late Eocene, and controlled the prototype formation of faulted block and faulted nose traps. The faulted traps were finally formed in the Middle and Late Oligocene, due to the weak activity of the faults. The faulted anticlinal traps associated with the arcuate faults F3 are distributed within the Pinghu and Huagang formations in the hanging wall of the fault. The hard linkage of arcuate fault F3, combined with the compressional stress of the Yuquan movement at the end of the Eocene, facilitated the formation of a flexural trap prototype within the Pinghu Formation in the hanging wall. Due to the strong compression during the Longjing movement at the end of the Miocene, the Yuquan Formation and the lower strata in the hanging wall of the fault were folded, and the amplitude of the fold in the Pinghu Formation increased. Subsequently, the faulted anticlinal trap controlled by F3 was finally formed. The structural traps formed by arcuate faults in the Tiantai slope represent favorable areas for hydrocarbon accumulation.

5.2. Controls of arcuate faults on reservoirs distribution

The segmentation growth processes of faults have significant implications for sedimentation and stratigraphic distribution. This paper focuses on the controls of the arcuate faults F1, F2, and F3 on the distribution of sedimentary facies within the upper member of the Eocene Pinghu Formation and the lower member of the Oligocene Huagang Formation.

Sediments of the upper member of the Pinghu Formation in the arcuate faults area were derived mainly from the Haijiao uplift, with additional contributions from the Yushan uplift. The sedimentary facies

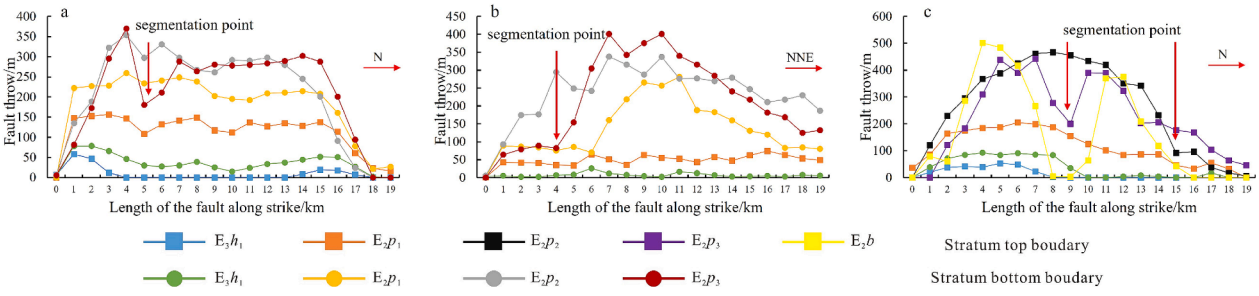

Fig. 5. The displacement-distance curve of the arcuate faults F1 (a), F2 (b), and F3 (c). The displacement-distance curve of fault is plotted by fault throws at different positions along fault strike. The red arrow indicates the segmentation point of arcuate faults.

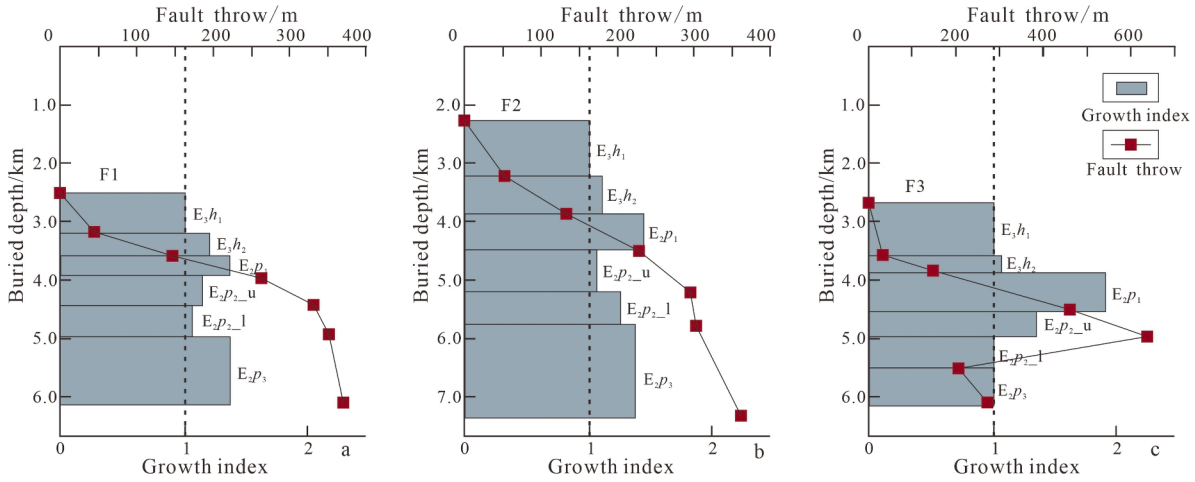

Fig. 6. Fault displacement buried depth curve and growth index curve of the Pinghu Formation and Huagang Formation during the depositional period of arcuate faults in the Tiantai slope. (a) Fault displacement buried depth curve and growth index curve of fault F1. (b) Fault displacement buried depth curve and growth index curve of fault F2. (c) Fault displacement buried depth curve and growth index curve of fault F3.

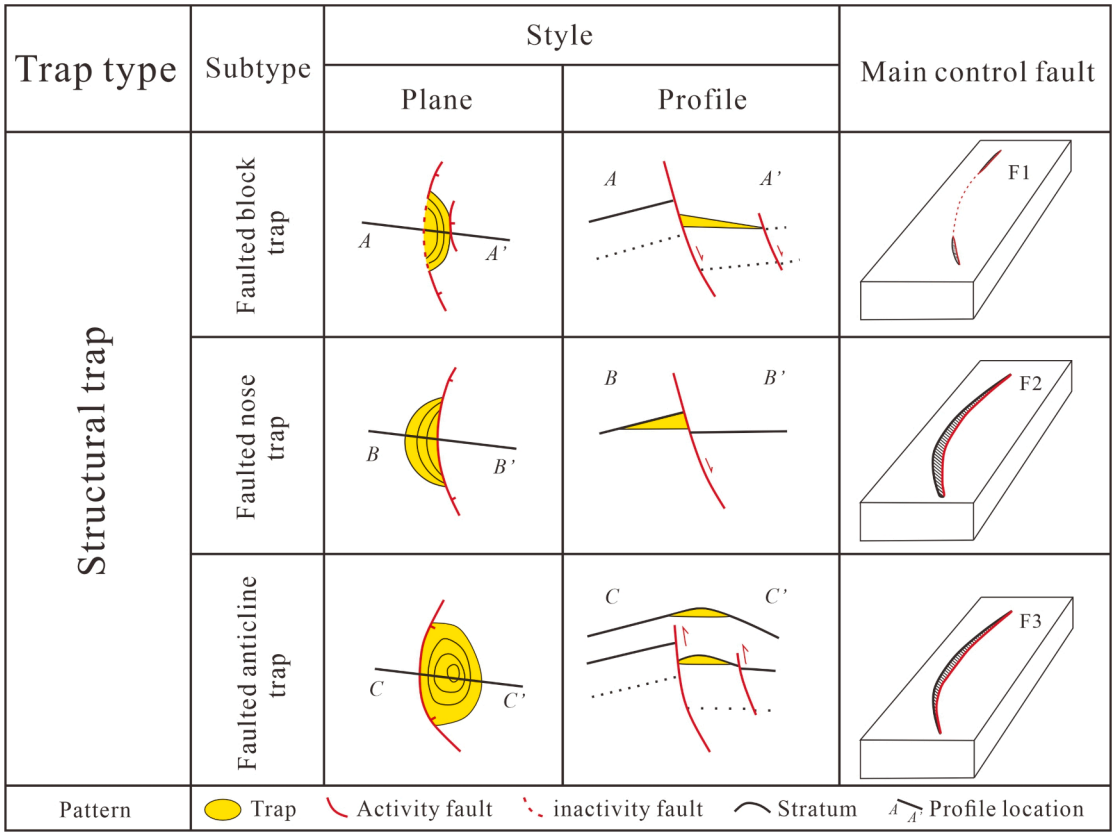

Fig. 7. Types of traps congtolled by the arcuate faults in the Tiantai slope.

of the upper member of the Pinghu Formation are characterized by delta plains and delta fronts, influenced by tidal processes. The variability in paleo-falls along the strikes and segmentation points of the arcuate faults markedly affected the transport pathways and accumulation sites of sandbodies. On the western side of arcuate fault F1, delta plains developed in the upper member of the Eocene Pinghu Formation. Distributary channels descended into the basin following the low topographies of the fault, and the transport channels for sandbodies flowed into the downstream areas through the segmentation points and the areas with low paleo-falls. From these positions, the sedimentary system changed into delta fronts, which propogated basinward and continued towards the low sags through low paleo-falls along the western sectors of arcuate faults F2 and F3, resulting in an overall arcuate distribution of sandbodies (Fig. 8a). In addition, the eastern part of the footwall of arcuate fault F1 hosted a series of sandbodies within the delta front. The subaqueous distributary channels of the delta front transported sandy sediments by the segmentation points and low paleo-fall zones of arcuate faults F2 and F3, depositing along the footwall strikes before accumulating in the low sags. As the delta front moved towards the basin, the tidal influence gradually increased. The tidal currents

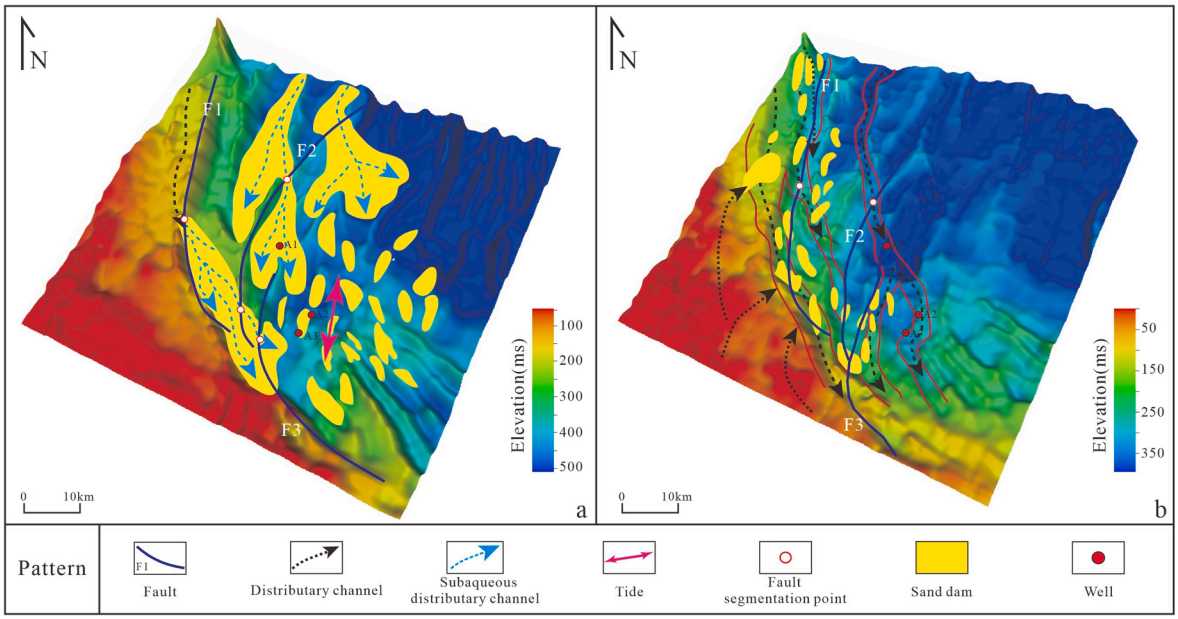

Fig. 8. Distribution map of palaeogeomorphology and sedimentary facies in the arcuate faults development area of the Tiantai slope. (a) Palaeogeomorphology and sedimentary facies distribution map of the upper section of the Eocene Pinghu Formation. (b) Paleogeomorphology and sedimentary facies distribution map of the lower section of the Oligocene Huagang Formation.

modified the sandbodies of the delta front, forming of tidal sand bars with discontinuous distributions (Fig. 8a).

During the depositional period of the lower member of the Oligocene Huagang Formation, the source materials for the arcuate fault zone originated from the Yushan uplift to the south and the Haijiao uplift to the north. The depositional environment was characterized by distributary channels within a delta plain setting. The arcuate faults controlled the spatial distribution of the distributary channels of the delta plain in the lower member of the Huagang Formation (Fig. 8b). The distributary channels entered the basin from the northern side of the arcuate faults, which were distributed along the faults strikes in most regions. Conversely, the southern side of the faults, characterized by lower terrain during the development stage of the delta plain, facilitated towards the southward extension of the distributary channels. At the northern segmentation points and locations with low paleo-falls of the arcuate faults F1, F2, and F3, the distributary channels intersected the faults at low angles, establishing new transport pathways for sandbodies. These sandbodies were mainly distributed on the descending walls of faults F1 and F3 (Fig. 8b). The increased accommodation space of the descending walls of the arcuate faults resulted in sediments thickening and sandbodies accumulation in the areas with low terrain.

In summary, the control mechanisms of arcuate faults on sandbody distribution can be divided into two primary models: sandbody accumulation within fault troughs and sandbody transport through fault segmentation points. Typically, fault troughs exhibit greater accommodation space, facilitating the development of distributary channels and subaqueous distributary channels along the fault strikes. This results in the deposition and accumulation of channel and delta front sandbodies within these troughs.

5.3. Controls of arcuate faults on hydrocarbon migration

The impact of faults on hydrocarbon migration are characterized by three aspects, involving the distribution of oil-source faults, the transport capacity of the faults, and the matching relationship between fault activity and the timing of hydrocarbon accumulation. For fault-controlled structural traps, the ability of oil and gas to migrate along faults and accumulate in the traps is mainly determined by the lateral sealing capability of the faults that govern trap formation (Sun et al., 2013). Specifically, when oil and gas migration occurs, if the fault controlling the trap formation has effective lateral sealing, oil and gas can accumulate and be preserved within the trap. Conversely, even if oil and gas are extensively introduced into the trap, they cannot be preserved if the fault lacks sufficient lateral sealing. In this study, the SGR (shale gouge ratio) method is used to evaluate the lateral sealing capacity of the arcuate faults (Lu et al., 2009b). According to the fault sealing evaluation parameters for the Pinghu oil–gas field in the northern side of the Tiantai slope (Zhang, 2012) and the SGR statistics for the arcuate faults, it has been determined that the lateral sealing capacity of the arcuate faults is stronger when the SGR $>$ 0.5, and weaker when SGR $<$ 0.5. The results show that the lateral sealing capacity of the northern sector of the arcuate fault F1 and the entire fault F2 was better during the depositional period of the upper member of the Pinghu Formation, whereas the bends of the fault F3 had a weaker lateral sealing ability. During the depositional period of the lower member of the Huagang Formation, the northern end of the fault F1 and the bends of the faults F2 and F3 demonstrated poor lateral sealing, while the other parts of the arcuate faults displayed strong on lateral sealing properties (Fig. 9). Consequently, the lateral sealing capacity of the arcuate faults was generally robust, promoting favorable conditions for hydrocarbon accumulation and preservation in the traps of the Pinghu and Huagang formations.

Since the Miocene, the source rocks of the Pinghu Formation have reached the peak of hydrocarbon generation (Lu et al., 2009a; Zhou, 2020; Qu et al., 2024), leading to vertical and lateral migration of hydrocarbons along faults and sandbodies, respectively. The arcuate faults served as key vertical migration pathways, allowing hydrocarbon to accumulate in traps within the upper member of the Pinghu Formation and the lower member of the Huagang Formation. Due to the sandbodies discontinuity, hydrocarbon were primarily accumulated in sandbodies located near the source rocks and oil-source faults. Traps located at relatively higher position were more likely to capture migrating hydrocarbon, resulting in the formation of various lithological reservoirs. In addition, thick sandbodies without associated traps acted as effective migration conduits, faciliting hydrocarbon migration to higher structural positions (Fig. 10).

The analysis of hydrocarbon generation and expulsion shows that there are two sets of source rocks developed in the Xihu Depression,

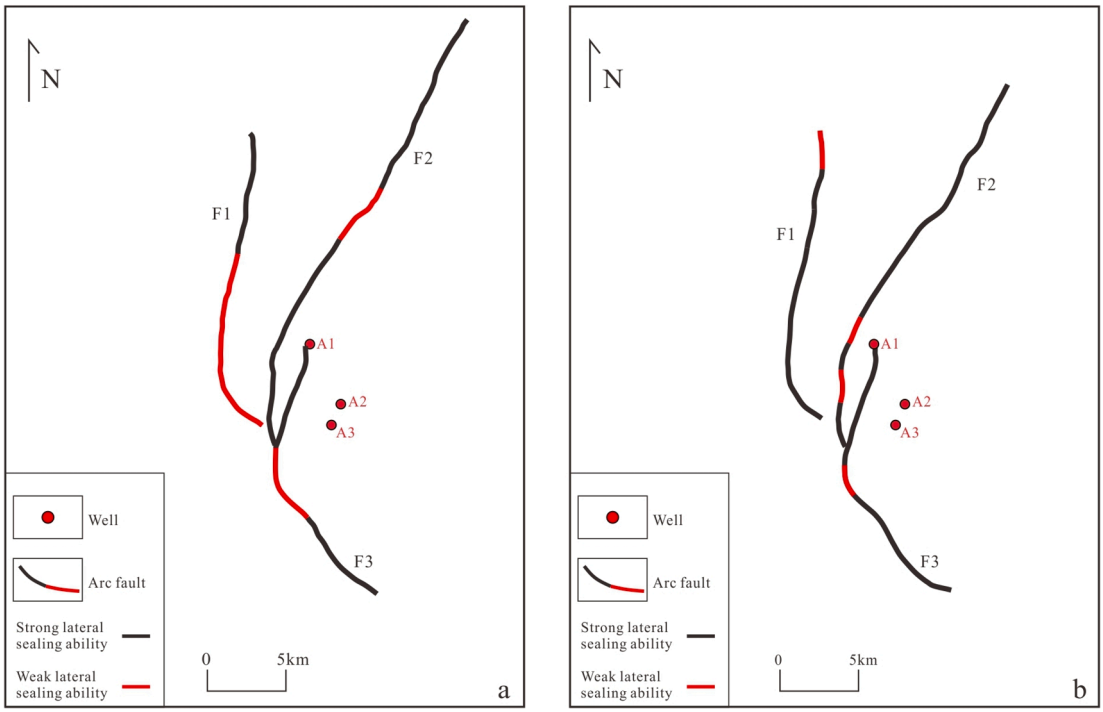

Fig. 9. Evaluation results of lateral sealing of ability of the arcuate faults on the top upper member of the Pinghu Formation (a), and on the top lower member of the Huagang Formation (b) in the Tiantai slope. Black and red line show that the fault has good and weak lateral sealing ability, respectively.

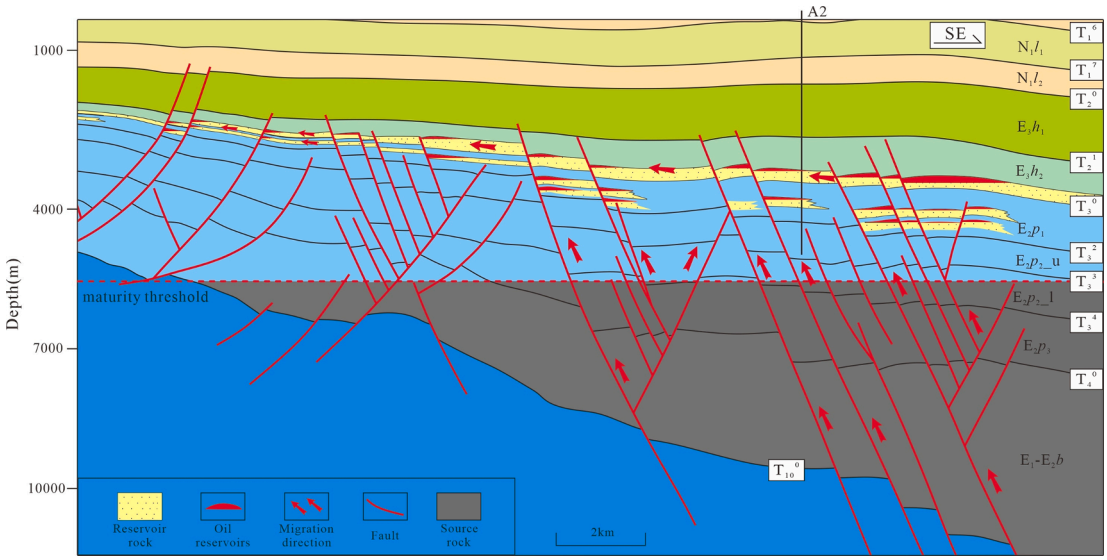

Fig. 10. Hydrocarbon accumulation model in the arcuate fault development area of the Tiantai slope.

including the Eocene Pinghu Formation and the Oligocene Huagang Formation (Liu et al., 2020). The source rocks in the Pinghu Formation began significan hydrocarbon generation toward the end of depositional stage of the Oligocene Huagang Formation, with this activity persisting to the present (Lian, 2018; Yu et al., 2022). Extensive hydrocarbon generation and expulsion from these effective source rocks occurred at the end of depositional stage of the Miocene Liulang Formation (Yu et al., 2018). According to the comprehensive analysis of the arcuate faults activity in the Tiantai slope, there was a good matching relationship between the periods of massive hydrocarbon generation and expulsion and the establishment of the traps; specifically, hydrocarbon generation and expulsion occurred after the trap formation. Therefore, the sandbodies within both the Pinghu and Huagang formations are conducive to hydrocarbon accumulation and subsequent formation of hydrocarbon reservoirs (Fig. 11).

6. Conclusion

The NW-trending pre-existing basement normal faults in the Tiantai slope experienced strike-slip movements during the Middle and Late Eocene, resulting in a change of the Cenozoic fault strikes in the hanging wall from NE to NW. The Cenozoic faults have arcuate-shaped distribution in plan view and control the deposition of the Pinghu Formation.

The evolution processes of the arcuate faults mainly can be divided into three stages, including the segmental growth stage in the Middle Eocene, the hard linkage growth stage in the Late Eocene, and the

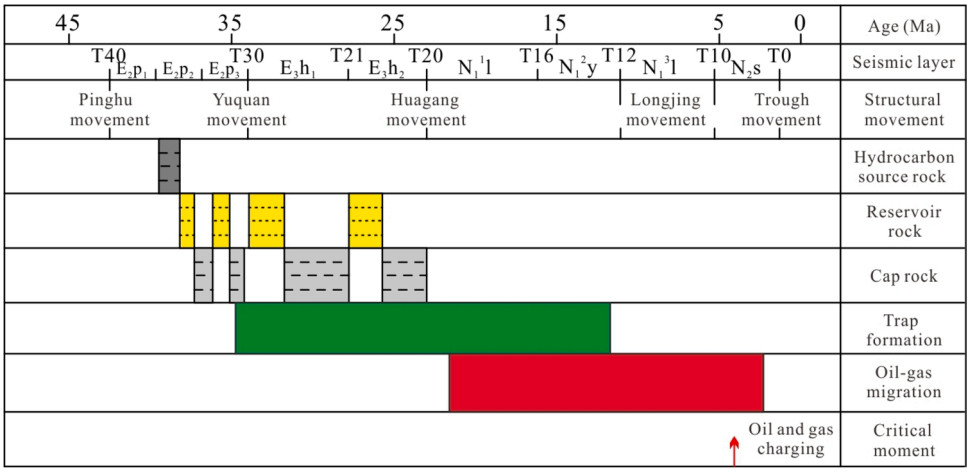

Fig. 11. Map showing hydrocarbon accumulation events in the Tiantai slope.

activity weakening stage in the Oligocene.

The hard linkage growth of the arcuate faults controlled the beginning of traps formation, and the traps were basically finally formed in the stage of activity weakening of the faults. The differential segmented growth of these arcuate faults exerted an important influence on the depositional thicknesses of the upper member of the Eocene Pinghu Formation and the lower member of the Oligocene Huagang Formation. Arcuate faults played a critical role in governing the development of the delta distributary channels, subaqueous distributary channels, and tidal sand bars during the depositional periods of the upper member of the Pinghu Formation and the lower member of the Huagang Formation. The accumulation of sandbodies occurred predominantly within fault troughs, facilitated by the transportion processes through fault segmentation points.

The arcuate faults in the Tiantai slope served as main pathways for vertical hydrocarbon migration. The lateral sealing capabilities of these faults were robust, effectively facilitating the accumulation of hydrocarbons in the structural traps proximal to these faults.

Credit authorship contribution statement

Lang Yu: Writing – original draft, Methodology, Data curation. **Yixin Yu:** Writing – review & editing, Supervision, Conceptualization. **Yiming Jiang:** Visualization, Conceptualization. **Wei Zou:** Visualization, Conceptualization. **Gongcheng Zhang:** Formal analysis. **Xianjun Tang:** Conceptualization. **Ting Tang:** Software, Investigation. **Xinxin Liang:** Investigation, Formal analysis. **Xinjian He:** Software, Investigation. **Dongxia Chen:** Supervision.

Declaration of competing interest

The authors declare that they have no known competing financial interests or personal relationships that could have appeared to influence the work reported in this paper.

Data availability

Data will be made available on request.

Acknowledgments

This work was jointly funded by the National Natural Science Foundation of China (Grant No. 42072149) and the Scientific Research Project of CNOOC (China) Limited (CNOOC-KJ135ZDXM39SH01). We thank the Research Institute of CNOOC Shanghai Branch for providing the data used in this study and the permission to publish the results. We are grateful to Gong Chenglin and Peng Yang for help in revision of the manuscript.

References

Bense, V.F., Berg, E.H.V.D., Balen, R.T.V., 2003. Deformation mechanisms and hydraulic properties of fault zones in unconsolidated sediments. the Roer Valey Rift System, The Netherlands. Hydrgeol. J. 11 (3), 319–332.

Cai, H., Zhang, J.P., 2013. Characteristics of faults on the Pinghu slope of XiHu Sag, the East China Sea Shelf Basin and their sealing capacity. Mar. Geol. Front. 29 (4), 20–26 in Chinese with English abstract.

Cai, H., Zhang, J.P., Tang, X.J., 2014. Characteristics of the fault systems and their control on hydrocarbon accumulation in the Xihu Sag, East China Sea Shelf Basin. Nat. Gas Ind. 34 (10), 18–26 in Chinese with English abstract.

Clague, D.A., Dalrymple, G.B., 1989. Tectonics, geochronology, and origin of the Hawaii-emperor chain. In: The Geology of North America, N. Geology Society of American, boulder, Colo., pp. 188–217.

Feng, Y.L., 2006. Control of valley and tectonic slope-break zone on sand bodies in rift-subsidence basin. Acta Pet. Sin. 27 (1), 13–16 in Chinese with English abstract.

Fossen, H., Schultz, R.A., Shipton, Z.K., Mair, K., 2007. Deformation bands in sandstone: a review. J. Geol. Soc. London 164 (4), 755–769.

Fossen, H., 2010. Structural geology.Cambridge University Press, New York, pp. 119~185.

Giba, M., Walsh, J.J., Nicol, A., 2012. Segmentation and growth of anobliguely reactivated normal fault. J. Struct. Geol. 39, 253–267.

Jiang, Y.M., Zou, W., Liu, J.S., Tang, X.J., He, X.J., 2020. Genetic mechanism of inversion anticline structure at the end of Miocene in Xihu Sag, East China Sea: a new understanding of basement structure difference. Earth Sci. 45 (3), 968–979 in Chinese with English abstract.

Jiao, R.C., 1988. On properties of Zhoushan-Guotou fault zone and its extension towards the continent. Geophys. Geochem. Explor. 12 (4), 249–255 in Chinese with English abstract.

Li, J.Y., Jiang, B., Qu, Z.H., Yin, S., Xu, J., Li, P., 2016. Tectonic evolution and control of coal in Donghai Xihu Sag. Coal Geol. Explor. 44 (5), 22–27 in Chinese with English abstract.

Lian, X.C., 2018. A model of hydrocarbon accumulation in deeply buried low permeability—high density sandstone gas reseryoirs in Xhu Sag, East China Sea. Mar. Geol. Front. 34 (2), 23–30 in Chinese with English abstract.

Liang, X.X., Chen, S., Ma, B.S., Ding, B.T., Liang, Y.Y., Song, X.G., Zhou, J.X., Yu, Y.X., Yu, L., 2024. Changes of tectonic regime of the East China Sea Shelf Basin since Mesozoic: insights from the Tiantai slope belt, East China Sea. J. Asian Earth Sci. 259, 105900.

Liu, J.S., Li, S.X., Qin, L.Z., Yi, Q., Chen, X.D., Kang, S.L., Shen, W.C., Shao, L.Y., 2020. Hydrocarbon generation kinetics of Paleogene coal in Xihu Sag, East China Sea Basin. Acta Pet. Sin. 41 (10), 1174–1187 in Chinese with English abstract.

Liu, Y.X., 2017. The Study on the evolution and genetic mechanism of fault system in the middle-shallow formations in northern Daqing Placanticline[dissertation]. Daqing: Northeast Petroleum University (in Chinese with English abstract).

Lu, Y.F., Huang, J.S., Fu, G., Fu, X.F., 2009b. Quantitative study on fault sealing ability in sandstone and mudstone thin interbed. Acta Pet. Sin. 30 (6), 824–829 in Chinese with English abstract.

Lu, J.Z., Ye, J.R., Huang, S.B., Wu, J., 2009a. Characteristics and hydrocarbon generation-expulsion histories of source rocks of Pingbei area in Xihu Depression. Offshore Oil. 29 (4), 38–43 in Chinese with English abstract.

Luo, Q., Bai, X.H., 1998. Fault controlling hydrocarbon theory and practice—study of fault activity and petroleum accumulation. Wuhan: China University of Geosciences Press (in Chinese with English abstract).

Peacock, D.C.P., Sanderson, D.J., 1994. Geometry and develoomment of relay ramps in normal fault systems. Am. Assoc. Petrol. Geol. Bull. 78 (2), 147–165.

Qu, T., Huang, Z.L., Li, T.J., Yang, Y.Z., Wang, B.R., Wang, R., 2024. Formation conditions and reservoir forming characteristics of the Wuyunting condensate gas field innorthern Pinghu slope zone of the Xihu sag. Acta Geol. Sin. 98 (1), 247–265 in Chinese with English abstract.
Ren, J.Y., Zhang, Q.L., Lu, Y.C., 2004. Arc-shaped fault break slope system and its control on low stand systems sandbodies in dongying depression. Acta Sedimentol. Sin. 22 (4), 628–635 in Chinese with English abstract.
Sample, J.C., Woods, S., Bender, E., Loveall, M., 2006. Relationship between deformation bands and petroleum migration in an exhumed reservoir rock Los Angeles Basin, California, USA. Geofluids 6 (2), 105–112.
Segall, P., Pollard, D.D., 1980. Mechanics of discontinuous faults. J. Geophys. Res. 85, 4337–4350.
Sun, Y.H., Qi, J.F., Lu, Y.F., Han, H.J., 2008. Characteristics of fault structure and its control to hydrocarbon in Bozhong Depression. Acta Pet. Sin. 29 (5), 669–675 in Chinese with English abstract.
Sun, Y.H., Zhao, B., Dong, Y.X., Zheng, X.F., Hu, M., 2013. Control of faults on hydrocarbon migration and accumulation in the Nanpu Sag. Oil Gas Geol. 34 (4), 540–549 in Chinese with English abstract.
Suo, Y.H., Li, S.Z., Dai, L.M., Liu, X., Zhou, L.H., 2012. Cenozoic tectonic migration and basin evolution in East Asia and its continental margins. Acta Petrol. Sin. 28 (8), 2602–2618 in Chinese with English abstract.
Taira, A., Okada, H., Whitaker, J.H., Smith, A.J., 1982. The Shimanto Belt of Japan: cretaceous-lower Miocene active-margin sedimentation. Geol. Soc. Lond. Spec. Publ. 10 (1), 5–26.
Wan, J.F., Xian, B.Z., Li, Z.P., Zhang, J.G., Jiang, Z.X., Wang, J.W., 2013. Different levels of rift activity and its impact on deposition in offshore area, Nanpu Sag. Acta Sedimentologica Sinica. 31 (6), 1059–1069 in Chinese with English abstract.
Wang, H.Y., Fu, X.F., Wang, H.X., Chen, M., Meng, L.D., Ping, G.D., 2020b. Research on the controlling effect of quantitative analysis and evaluation of fault activity on oil and gas accumulation in Qikou sag of Bohai Bay Basin. Acta Geol. Sin. 94 (10), 3062–3073 in Chinese with English abstract.
Wang, H.X., Li, M.H., Shen, Z.S., Fu, X.F., Cheng, Z.Y., Wang, B., 2014. The establishment and geological signifcance of quantitative discrimination criterion of fault segmentation growth—an example from saertu reservoir in Xingbei development area of Songliao Basin. Geol. Rev. 60 (6), 1259–1264 in Chinese with English abstract.
Wang, J.H., Liu, L.H., Chen, S.H., Shang, Y.L., 2011. Tectonic-sedimentary responses to the second episode of the Zhu-Qiong movement in the Enping Depression, Pearl River Mouth Basin and its regional tectonic significance. Acta Pet. Sin. 32 (4), 588–595 in Chinese with English abstract.
Wang, X.Y., Liu, Q.H., Zhu, H.T., Hou, G.W., Qin, L.Z., 2021. 3-D engraving of volcanic mechanism in the Tiantai slope of Xihu Depression and its formation mechanism. Bull. Geol. Sci. Technol. 40 (4), 72–80 in Chinese with English abstract.
Wang, C., Tang, X.J., Jiang, Y.M., He, X.J., Tan, S.Z., 2020a. Characteristics of the structural transfer zone of northern Tiantai slope in Xihu Sag of the East China Sea Basin and their petroleum geological significances. Mar. Geol. Quat. Geol. 40 (6), 93–105 in Chinese with English abstract.
Wilson, D.S., 2016. Revision of Paleogene plate motions in the Pacific and implications for the Hawaiian-Emperor bend: comment. Geology 44 (4), e384.
Wu, Z.Y., Wang, X.B., Jin, X.L., Li, J.B., Gao, J.Y., 2004. The evidences of the backarc spreading and discussion on the key issues in the Okinawa Trough. Mar. Geol. Quat. Geol. 24 (3), 67–76 in Chinese with English abstract.
Wu, Z., Wu, T.T., Wang, W.Y., Zhang, Z.T., Xu, X.M., Yu, S.M., 2020. The study on fault controlling petroleum accumulation in enping sag of pearl river mouth basin. J. Yangtze Univ. (Nat. Sci. Edit.). 17 (5), 18–24 in Chinese with English abstract.
Yang, W.D., Cui, Z.K., Zhang, Y.B., 2010. Geology and Mineral Resources of the East China Sea. Beijing, China Ocean Press (in Chinese with English abstract).
Yielding, G., Freeman, B., Needham, D.T., 1997. Quantitative Fault Seal Prediction. AAPG Bull. 81 (6), 897–917.
Yu, Z.K., Ding, F., Zhao, H., 2018. Characteristics of structural evolution and classification of hydrocarbon migration and accumulation units in Xihu Sag China. Shanghai Land Resour. 39 (4), 75–78 in Chinese with English abstract.
Yu, L., Yu, Y.X., Jiang, Y.M., Zou, W., Chen, S., Tang, X.J., Liang, X.X., He, X.J., Chen, D. X., 2023. Characteristics and forming mechanisms of transform zone in the Tiantai slope, Xihu Sag, East China Sea Shelf Basin. Oil Gas Geol. 44 (3), 753–763 in Chinese with English abstract.
Yu, Y.F., Zhang, J.P., Cheng, C., Tang, X.J., Xu, H.Z., 2022. Main controlling factors and reservoir forming model for hydrocarbon accumulation in the Xihu Sag, the East China Sea Shelf Basin. Mar. Geol. Front. 38 (7), 40–47 in Chinese with English abstract.
Zhang, J., 2012. Study on fault-sealing in Pinghu oil and gas field, Xihu Depression. Petrol. Geol. Rec. Efficiency 19 (4), 18–20 in Chinese with English abstract.
Zhang, J.P., 2013. Fault system and its genetic mechanism in the Pinghu slope of the Xihu Sag in the East China Sea Shelf Basin. Chinese J. Geol. 48 (1), 291–303 in Chinese with English abstract.
Zhang, S.L., Zhang, J.P., Tang, X.J., Zhang, T., 2014. Geometry characteristic of the fault system in Xihu Sag in East China Sea and its formation mechanism. Mar. Geol. Quat. Geol. 34 (1), 87–94 in Chinese with English abstract.
Zhang, X.Q., Zhang, G.C., Jiang, Y.M., Cui, M., He, X.J., 2023. The control of curved faults on structural trap formation: Tiantai slope belt, Xihu Sag, East China Sea. Mar. Pet. Geol. 156, 106464.
Zhou, X.H., 2020. Geological understanding and innovation in Xihu Sag and breakthroughs in oil and gas exploration. China Offshore Oil Gas. 32 (1), 1–12 in Chinese with English abstract.
Zhou, X.H., Jiang, Y.M., Tang, X.J., 2019. Tectonic setting, prototype basin evolution and exploration enlightenment of Xihu Sag in East China Sea basin. China Offshore Oil Gas. 31 (3), 1–10 in Chinese with English abstract.
Zhu, B.H., Xie, C.Y., Liu, M., Zhu, L.X., 2022. Fault characteristics and analvsis of controlling factors on sedimentation and trap formation in Pinabei area of Xihu Depression. Offshore Oil. 42 (3), 1–10 in Chinese with English abstract.
Zou, W., Yu, Y.X., Liu, J.S., Jiang, Y.M., Tang, X.J., Chen, S., Yu, L., 2021. Main controlling factors of the central inversion structure belt and the development of Ningbo anticline in Xihu Sag, East China Sea Basin. Acta Pet. Sin. 42 (2), 176–185 in Chinese with English abstract.